VI.　研究成果の刊行に関する一覧表

別紙４

研究成果の刊行に関する一覧表

書籍

著者氏名	論文タイトル名	書籍全体の編集者名	書　籍　名	出版社名	出版地	出版年	ページ
Hirata M, Kishima H, Yanagisawa T, Taniguchi M, Hosomi K, Goto T, Yoshimine T, Okinaga T, Shimono S, Imai K	Brain–Machine Interface Using Brain Surface Electrodes: Real-Time Robotic Control and a Fully Implantable Wireless System	Go R	In Biomedical Engineering and Cognitive Neuroscience for Healthcare; Interdisciplinary Applications	IGI Global	USA	2013	pp362-374

雑誌

発表者氏名	論文タイトル名	発表誌名	巻号	ページ	出版年
Hirata M, Yoshimine T	Clinical application of neuromagnetic recordings:from functional imaging to neural decoding	IEICE Trans Electron	96(3)	313-319	2013
Nomura K, Kazui H, Tokunaga H, Hirata M, Goto T, Goto Y, Hashimoto N, Yoshimine T, Takeda M	Possible roles of the dominant uncinate fasciculus in naming objects: A case report of intraoperative electrical stimulation on a patient with a brain tumour	Behav Neurol			In press
Yanagisawa T, Yamashita O, Hirata M, Kishima H, Saitoh Y, Goto T, Yoshimine T, Kamitani Y	Regulation of motor representation by phase-amplitude coupling in the sensorimotor cortex	J Neurosci.	32(44)	15467-75	2012
Hosomi K, Kishima H, Oshino S, Hirata M, Tani N, Maruo T, Khoo HM, Shimosegawa E, Hatazawa J, Kato A, Yoshimine T	Altered extrafocal iomazenil activity in mesial temporal lobe epilepsy	Epilepsy Res	103(2-3)	195-204	2013

Sugata H, Goto T, Hirata M, Yanagisawa T, Shayne M, Matsushita K, Yoshimine T, Yorifuji S	Neural decoding of unilateral upper limb movements using single trial MEG signals	Brain Res.	1468	29-37	2012
平田雅之、亀山茂樹、後藤 哲、柳澤琢史、貴島晴彦、押野 悟、吉峰俊樹、井口義信、石井良平、尾﨑 勇、鎌田恭輔、白石秀明、露口尚弘、渡辺裕貴、橋本 勲	脳磁図の臨床応用に関する文献レビュー(第1報)：てんかん	臨床神経生理学	40（3）	140-146	2012
平田雅之、柳澤琢史、松下光次郎、後藤哲、菅田陽怜、モリスシェイン、影山悠、貴島晴彦、齋藤洋一、吉峰俊樹	Brain-machine interfaceの進歩	分子脳血管病	11(3)	16-23（252-259）	2012
平田雅之、柳澤琢史、松下光次郎、モリスシェイン、神谷之康、鈴木隆文、吉田毅、佐藤文博、齋藤洋一、貴島晴彦、後藤哲、影山悠、川人光男、吉峰俊樹	ブレイン・マシン・インターフェースによる機能支援：リアルタイムロボットアーム制御とワイヤレス完全体内埋込装置の開発	脳神経外科ジャーナル	21(7)	541-549	2012
露口尚弘、鎌田恭輔、中里信和、宇田武弘、池田秀敏、坂本真一、尾崎勇、井口義信、平田雅之、亀山茂樹、石井良平、白石秀明、渡辺裕貴、橋本勲	脳磁図の臨床応用に関する文献レビュー(第2報)：虚血性脳血管障害	臨床神経生理学	40（4）	195-202	2012
白石秀明、尾崎勇、井口義信、石井良平、鎌田恭輔、亀山茂樹、露口尚弘、中里信和、平田雅之、渡辺裕貴、橋本勲	脳磁図の臨床応用に関する文献レビュー(第3報)：小児疾患	臨床神経生理学	40（4）	203-208	2012
平田雅之	低侵襲型BMIが拓く新たな可能性	地域リハビリテーション	7	940-943	2012
平田雅之	ブレイン・マシン・インターフェース（BMI）とリハビリテーション	理学療法学	39(8)	503-509	2013

石井良平、渡辺裕貴、青木保典、平田雅之、白石秀明、尾崎勇、井口義信、露口尚弘、鎌田恭輔、亀山茂樹、中里信和、橋本勲、武田雅俊	脳磁図の臨床応用に関する文献レビュー(第4報)：精神科疾患・認知症	臨床神経生理学	41(1)	29-45	2013
鎌田恭輔、露口尚弘、中里信和、尾崎勇、池田英敏、井口義信、平田雅之、亀山茂樹、石井良平、白石秀明、渡辺裕貴、橋本勲	脳磁図の臨床応用に関する文献レビュー(第5報)：脳腫瘍	臨床神経生理学	41(1)	46-53	2013
平田雅之、吉峰俊樹	ブレイン・マシン・インターフェース	再生医療　日本再生医療学会雑誌	12(1)	33-49	2013
平田雅之、吉峰俊樹	ブレイン・マシン・インターフェース	検査と技術	41(2)	147-151	2013
平田雅之、栁澤琢史、松下光次郎、菅田陽怜、モリス　シェイン、神谷之康、鈴木隆文、吉田毅、佐藤文博、森脇崇、梅垣昌士、齋藤洋一、貴島晴彦、影山悠、川人光男、吉峰俊樹	ブレイン・マシン・インターフェースの基礎と臨床応用	脳神経外科ジャーナル	22(3)	192-199	2013
Yorifuji S, Hirata M, Goto T, Okazaki A, Takahashi A, Sugata H, Onodera A, Hosokawa S	Present status and future development of neurophysiological examination in laboratory medicine	Rinsho Byori	60(9)	900-903	2012
尾崎勇、井口義信、白石秀明、石井良平、平田雅之、露口尚弘、鎌田恭輔、渡辺裕貴、亀山茂樹、橋本勲	脳磁図の臨床応用に関する文献レビュー(第6報)：神経変性・脱髄疾患と神経リハビリテーション	臨床神経生理学	41(2)	57-70	2013
Ota Y, Takura T, Sato F, Matsuki H	Wireless Power Transfer by Low Coupling Electromagnetic Induction — LC booster	IMWS-IWPT 2012 Proceedings		175-178	2012

小池健太，岩崎圭祐，加藤健太郎，田倉哲也，佐藤文博，佐藤忠邦，松木英敏	直接給電FES用給電アンテナの出力安定化に関する基礎検討	平成24年度電気関係学会東北支部連合大会 講演論文集		1H02（CD-ROM）	2012
佐藤圭太，森下壮一郎，加藤龍，横井浩史，梅田達也，渡辺秀典，西村幸男，伊佐正	硬膜下電位からのサル捕食運動中の状態判別とロボットアーム動作決定	日本ロボット学会誌	Vol. 31，No.1	pp.1-9	2013

Ⅶ.　研究成果の刊行物・別刷

Chapter 36
Brain-Machine Interface Using Brain Surface Electrodes:
Real-Time Robotic Control and a Fully Implantable Wireless System

Masayuki Hirata
Osaka University Medical School, Japan

Hiroshi Yokoi
The University of Tokyo, Japan

Takufumi Yanagisawa
Osaka University Medical School, Japan

Tetsu Goto
Osaka University Medical School, Japan

Kojiro Matsushita
Osaka University Medical School, Japan

Morris Shayne
Osaka University Medical School, Japan

Hisato Sugata
Osaka University Medical School, Japan

Youichi Saitoh
Osaka University Medical School, Japan

Yukiyasu Kamitani
ATR Computational Neuroscience Laboratories, Japan

Haruhiko Kishima
Osaka University Medical School, Japan

Takafumi Suzuki
The University of Tokyo, Japan

Mitsuo Kawato
ATR Computational Neuroscience Laboratories, Japan

Toshiki Yoshimine
Osaka University Medical School, Japan

ABSTRACT

The brain-machine interface (BMI) enables us to control machines and to communicate with others, not with the use of input devices, but through the direct use of brain signals. This chapter describes the integrative approach the authors used to develop a BMI system with brain surface electrodes for real-time robotic arm control in severely disabled people, such as amyotrophic lateral sclerosis patients. This integrative BMI approach includes effective brain signal recording, accurate neural decoding, robust robotic control, a wireless and fully implantable device, and a noninvasive evaluation of surgical indications.

DOI: 10.4018/978-1-4666-2196-1.ch036

INTRODUCTION

The brain-machine interface (BMI) is a man-machine interface that enables us to control machines and to communicate with others not with the use of input devices, but through the direct use of brain signals alone (Figure 1). Several diseases and conditions can lead to the loss of muscular control without a disruption in patients' brain function, including amyotrophic lateral sclerosis (ALS), brainstem stroke, spinal cord injury, and muscular dystrophy, among others. BMI technology offers these patients greater independence and a higher quality of life by enabling the control of external devices to communicate with others and the ability to manipulate their environment at will (Wolpaw, Birbaumer, McFarland, Pfurtscheller, & Vaughan, 2002).

There are two types of BMI: invasive BMI and noninvasive BMI. Invasive BMI requires surgical procedures and measures the brain signals from intracranial electrodes (needle electrodes or brain surface electrodes), whereas noninvasive BMI measures brain signals noninvasively from outside of the body using scalp electrodes, and so forth. To achieve a higher performance and a higher level of usefulness, we employed invasive BMI techniques, which involve the implantation of devices. For use in a practical situation, invasive BMI requires an organic integration of the following medical and engineering technologies:

1. Neural recording with high spatiotemporal resolution.
2. High-speed data transfer and processing.
3. Optimal extraction of appropriate neurophysiological features.
4. Accurate neural decoding.
5. Robust control of external devices such as robotic arms and electric wheelchairs.
6. Downsizing, integration, and implantation of electronic devices, and the use of wireless technology.
7. Noninvasive pre-surgical evaluations for appropriate surgical indications.
8. On-target survey and analysis of patient needs.
9. Addressing of neuroethical issues.

In this chapter, we describe the development of our invasive BMI system using brain surface electrodes.

Figure 1. A conceptual diagram of the brain machine interface

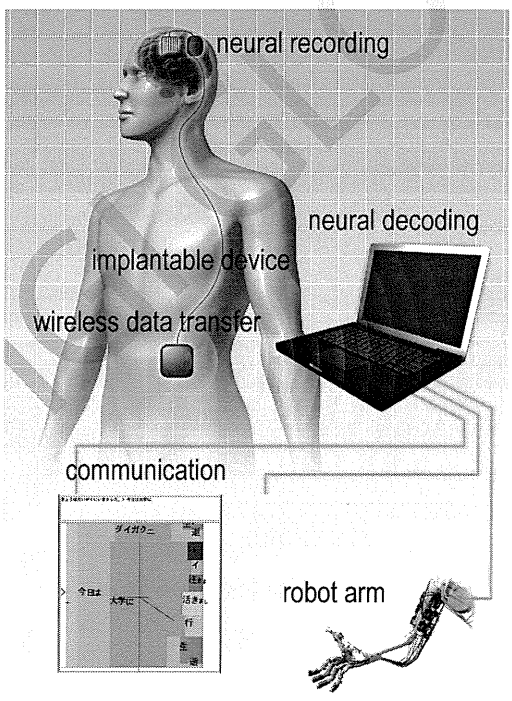

NEURAL DECODING AND REAL-TIME ROBOTIC CONTROL USING ELECTROCORTICOGRAMS

Clinical Studies Using Electrocorticograms Recorded from Brain Surface Electrodes

In the process of providing neurosurgical treatments for specific groups of patients, we some-

times record brain signals (electrocorticograms: ECoGs) or electrically stimulate the brain using electrodes that are directly placed on the brain surface. The ECoGs can selectively measure brain signals within a limited distance of a few millimeters without distortion. In addition, the ECoGs are insusceptible to external noises, and the scalp skin electrodes measure the distorted brain signals (electroencephalograms: EEGs) from a distance of up to a few centimeters. Furthermore, ECoG recordings from the brain surface electrodes are stable for at least one year (Chao, Nagasaka, & Fujii, 2010), whereas the spike recordings from the needle electrodes will gradually deteriorate in yield due to chronic inflammatory tissue reactions. The ECoG is a well-balanced brain signal for BMI (Table 1). Thus, we prefer to use the ECoGs recorded by the brain surface electrodes for BMI to achieve a high performance.

In our clinical studies, all of the subjects were recruited from patients in whom we temporarily placed brain surface electrodes to treat intractable pain or epilepsy. Informed consent was obtained from all of the patients, and all of the studies were performed with the approval of the ethics committee of Osaka University Medical Hospital. We measured the ECoGs during the performance of two or three types of simple motor tasks of the hand or arm, such as grasping, pinching, and elbow flexion. We predicted the type of movement based on the analysis of a single ECoG trial using a support vector machine (SVM) algorithm (Kamitani & Tong, 2005). As a result, we were able to predict movement types on a single trial basis with an accuracy rate of 70-90%. Specifically, we first demonstrated that ECoGs from the anterior wall of the central sulcus (a groove in the brain where most of the primary motor cortex lies) are useful for the accurate and early decoding of movement types (Yanagisawa et al., 2009). Most of the primary motor cortex, which is responsible for the final functional output of motor commands, lies within the anterior wall of the central sulcus. In humans, the anterior wall of the central sulcus contains many neurons that directly project to the spinal anterior horn cells, and such neurons are thought to be related to fine movement control (Rathelot & Strick, 2009). We suggest that an appropriate neurophysiological feature extraction from the central sulcus contributed to our accurate movement decoding.

Table 1. Brain signals used for the brain-machine interface

	Measured physiological phenomena	Spatial coverage	Spatial resolution	Temporal resolution	Time delay	Invasiveness	Long term recording stability	Portability
fMRI	CBF	whole brain	○ 3–5mm	× 4–5s	×4–5S	◎	○	×
NIRS	CBF	cortex	× 2cm	× 4–5s	×4–5S	◎	○	○
EEG	Neural activities	whole brain	× 3–4cm	○ 1ms	◎ 0	◎	○	○
MEG	Neural activities	cortex	△5–10mm	◎ 0.1ms	◎ 0	◎	○	×
ECoG	Neural activities	100cm²	○ 2–3mm	◎ 0.1ms	◎ 0	△	◎	◎
LFP	Neural activities	1cm²	○ 1mm	◎< 0.1ms	◎ 0	×	△	◎
spike	Neuronal activities	1cm²	◎ 0.2mm	◎< 0.1ms	◎ 0	×	×	◎

Figure 2. A real-time BMI system for robotic arm control

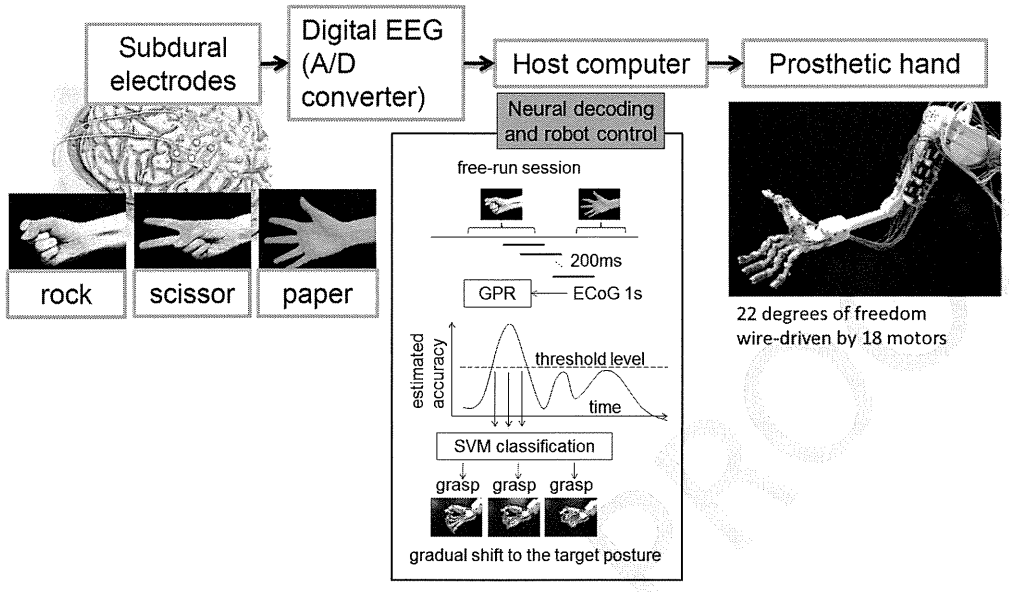

We applied this decoding method to an ECoG-based BMI system for real-time control of a robotic arm (Figure 2). The ECoGs were measured using a 128-channel digital EEG system (EEG 2000; Nihon Koden Corporation, Tokyo, Japan) and digitized at a sampling rate of 1000 Hz. We introduced successive decoding every 200 ms, and the Gaussian process regression was used to predict the movement onset. Next, the SVM was used to infer the type of hand and arm movements. The robotic arm was an experimental anthropomorphic hand developed by Prof. Yokoi H(Yokoi, Kita, & Nakamura, 2009). The general movement mechanisms and degrees of freedom of the hand mimicked those of a human hand. In addition, the hand was equipped with 8 DC motors to independently actuate 8 individual tendons in the robotic hand. The 8 tendons functioned in a coordinated manner to accomplish flexion or extension of each individual finger. As a result, we found that the normalized power in the high gamma band (80 - 150 Hz) gave the highest decoding accuracy of all the frequency bands and ranged from 3 to 150 Hz (Yanagisawa et al., 2011). We succeeded in generating the voluntary control of grasping and releasing of objects (Figure 3) (Yanagisawa et al., in press). Using a successive decoding and control algorithm, a smooth

Figure 3. Real-time control of a robotic arm. The patient voluntarily controlled grasping (right) and opening (left) of the robotic arm in real time.

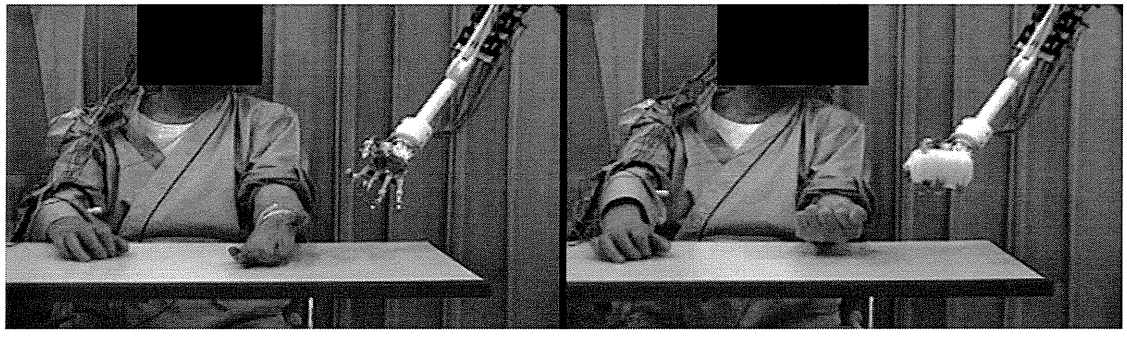

robotic hand movement was achieved, although the decoding accuracy on a single trial basis was approximately 70%. We found that despite being severely paralyzed, just the imagery of the hand movement could induce clear, high gamma band responses that were similar to those induced by real movements.

A FULLY IMPLANTABLE WIRELESS SYSTEM

Wired leads, which penetrate the skin, pose a high risk of infection. It is necessary to fully implant a recording system within the body to reduce the infection risk from the penetration of wire leads. Moreover, once the devices are implanted, it will be more convenient to use the BMI system because the patients would not have to wear or remove the system. For this reason, we have developed the first prototype of a fully implantable ECoG recording system for human brain-machine interfaces using brain surface electrodes. By integrating this wireless system into a real-time BMI system, we ultimately aim to develop a Wireless Human ECoG-based Real-time BMI System (W-HERBS) (Hirata et al., 2011).

System Overview

The first prototype is shown in Figure 4. This fully implantable system includes many new technologies such as a 64-ch integrated analog amplifier chip, a Bluetooth wireless data transfer circuit, a wirelessly rechargeable battery, 3-dimensional tissue conformable high-density electrodes, a titanium head casing, and a fluorine polymer body casing.

The implantable system consists of two parts; a head part and a body part. The head part consists of tissue conformable brain surface microelectrodes, a titanium head casing that also functions as an artificial skull, and a 128-ch amplifier unit with 2 64-ch chips. The body part consists of a wireless data transfer unit and a microchip data controller, a wireless rechargeable unit, and a fluorine polymer body casing.

Figure 4. A: The first prototype of a fully implantable wireless system for the W-HERBS. A fluorine polymer body casing, which includes a wireless rechargeable unit and a wireless data transfer unit (a). A titanium head casing / artificial skull (b). Brain surface microelectrodes conformable to the outer surface of the individual brain (c). Brain surface microelectrodes conformable to the brain groove (d). B: The prototype is attached to the skull bone model.

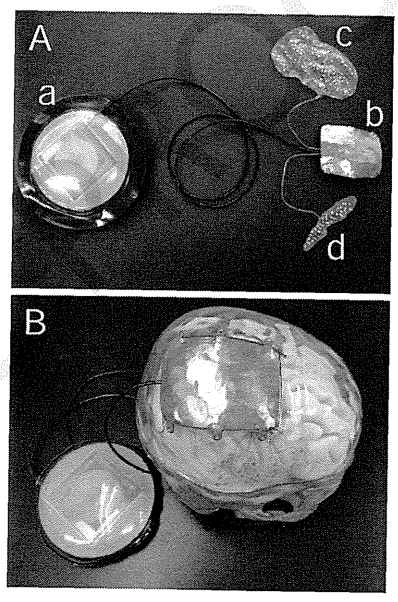

Integrated Analog Amplifier Unit

The ECoG is characterized as signals with low frequency bands that range from 0.1 Hz to 500 Hz and produces small amplitudes that range from 1 μV to 1 mV. It is necessary to reduce the input-referred noise of the amplifier to record the ECoG signals (Yoshida et al., 2010). The variable bandwidth and wide dynamic ranges are also important because commercial AC noises with similar frequency bands can easily contaminate ECoG signals. Thus, a high-linearity low noise amplifier with a variable bandwidth was developed to cover the frequency bands and voltage gains

appropriate for recording ECoG signals (Yoshida et al., 2011). The low noise amplifier with a 0.1 Hz roll-off frequency was implemented with core differential amplifiers using large-sized MOSFETs and a capacitor feedback scheme biased by ultra-high resistors of cascade 12 MOSFETs. A VLSI chip was fabricated using CMOS 0.18 μm process technology in the chip fabrication program of the VLSI Design and Education Center (VDEC) at the University of Tokyo.

The specifications of the chip functions are as follows:

- Number of channels: 64 channels.
- 12 bits A/D converter.
- Voltage gain: 40 – 80 dB.
- Signal frequency bands: 0.1 – 1000 Hz.
- Input referred noise: 2.8 μV.
- Power consumption: 4.9 mW.
- Chip size: 5.0 mm x 5.0 mm.
- Master/slave function for a 128-channel system.

A 128-channel analog amplifier board consists of two chips mounted on two high-density printed boards that were bridged by flexible printed wiring (Figure 5). The size of the board was 20 mm x 30 mm x 2.5 mm, which was small enough to be placed within a head casing, which will be described later in the text.

Figure 5. A 128-channel integrated analog amplifier board

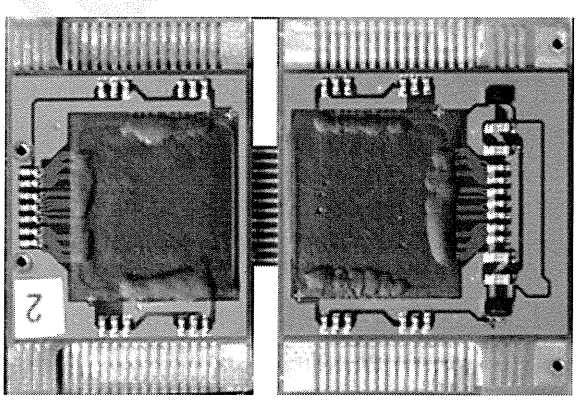

Wireless Data Transfer Unit

We adapted the Bluetooth protocol communication (Class 2) for the first prototype for its high usability. A combination of 2 sets of Bluetooth circuits enabled us to achieve effective data transmission rates of 400 kbps, which allowed the transfer of 128-ch x 12-bit ECoG data in real time. Power consumption was approximately 300 mW, which meant that most of the system power was consumed by the wireless data transfer. Further improvements in the data transfer protocol should be made to achieve a faster and more power-efficient operation of the system. The size was 60 mm x 60 mm x 8 mm, which should also be reduced. One solution would be to change the data transfer protocol from Bluetooth to WLAN or UWB.

Wireless Rechargeable Unit

The wireless battery charging system consists of two parts. One is a transmitter positioned outside of the human body, and the other is a receiver located inside the human body. We achieved a wireless charging power of 4 W at a distance of 38 mm, which was sufficient to run the entire implantable system. The coil size of the abdominal portion was 40 mm in diameter and 8 mm in thickness, which may be scaled down if the power consumption can be reduced.

Tissue Conformable Brain Surface Microelectrodes

To record the ECoGs with a higher spatiotemporal resolution, we developed 3-dimensional high-density grid electrodes, which were designed to fit to the individual's brain surface (Hirata et al., 2010). We extracted 3-dimensional (3D) surface data of the brain surface and brain groove from the patient's individual magnetic resonance (MR) images. An automatic brain groove extraction software program (Brain VISA, http://brainvisa.

Figure 6. Tissue conformable brain surface microelectrodes. The tissue conformable brain surface microelectrodes fitted on to the individual brain surfaces. Left: High-density electrodes (inter-electrode spacing 2.5 mm) and standard electrodes (inter-electrode spacing 10 mm). Middle: Gyral (brain surface) electrodes. Right: Sulcal (brain groove) electrodes.

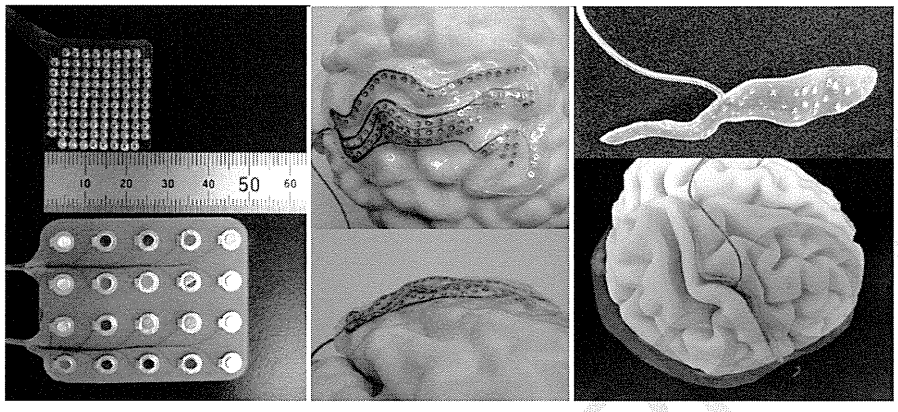

info/) was used. Next, we designed male and female molds for the grid electrodes using 3D CAD software (3 matic, Materialize Japan, Tokyo, Japan) (Figure 6). Next, the molds were rapidly produced by a 3D printer. The silicon sheets fitting the brain surface were subsequently produced from these molds. In addition, the location of each platinum electrode (1.0 mm in diameter) was designed with the 3D CAD software, which took into account the individual's anatomical information. The inter-electrode spacing was up to 2.5 mm and the brain groove grid electrodes were located on both sides of the electrode sheet. These 3D grid electrodes fitted onto the brain surface with only a minimal compression of the brain tissue and generated high ECoGs yields due to their close contact with the brain surface.

Head Casing and Artificial Skull Bone

We developed a titanium head casing, which contained a 128-channel amplifier unit. This casing functioned as both a head casing and an artificial skull bone and was designed to fit a patient's individual skull bone shape using the 3D CAD (3 matic, Materialize Japan, Tokyo) and 3D CAM (Gibbs CAM, Gibbs and Associates, USA) software programs (Figure 7). This head casing not only had cosmetic advantages, but it was also safer than other convex shapes that posed a higher risk of cutaneous fistula.

Fluorine Polymer Body Casing

Compared with the head casing, the body casing offers a larger space and does not require careful cosmetic consideration. We introduced a soft casing made of fluorine polymer, which has advantages in terms of cost, chemical stability, durability, and biocompatibility. This body casing embeds a wireless data transfer unit and a microchip data controller, a wireless power supply unit, and a rechargeable battery in silicone covered by fluorine polymer films.

NONINVASIVE NEURAL DECODING USING MAGNETOENCEPHALOGRAPHY

A noninvasive evaluation of the individual BMI performance is indispensable for determining the surgical indication of the invasive BMI treat-

Figure 7. A titanium head casing / artificial skull bone. A: A computer simulation of machining path using 3D CAM software. B: A computer simulation of a head casing fitting the skull bone. Left: skull bone opening. Middle: Outer side view of a head casing fitting the skull bone. Right: Inner side view. C: A head casing designed using 3D CAD software. Upper: A head casing without an electronic circuit board. Lower: A head casing with an electronic circuit board. D: A prototype casing. Upper: inner side view. Lower: outer side view. E: A prototype casing attached to the skull bone model. Three-dimensional skull bone data were obtained from the individual's CT images. The head casing contains two 64-channel integrated amplifier chips on a small mounting board, which was mounted onto a folded inner panel as indicated by the green color.

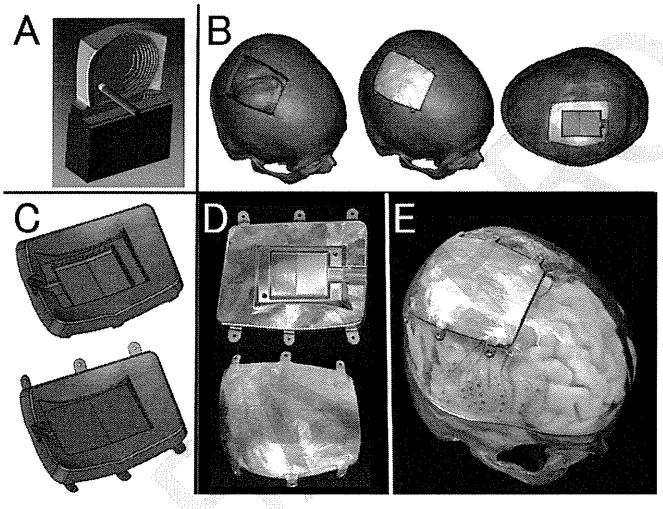

ment. A magnetoencephalography (MEG) is a potentially noninvasive method for evaluating individual BMI performance because of its high spatiotemporal resolution and neurophysiological compatibility with the ECoG. We investigated the neural decoding performance of 3 types of unilateral hand and arm movements on a single trial basis using an MEG (Sugata et al., 2012). We used an SVM to decode the movement types. The peak amplitudes of the first component after the movement onset of the movement-related cortical fields (pMRCF) were used as decoding features. As a result, the neural decoding accuracies largely exceeded the chance level in all of the 9 healthy subjects that were evaluated. The pMRCFs and decoding accuracies were strongly correlated ($rs = 0.900$, $p = 0.002$) (Figure 8). These results suggested that the neurophysiological profiles might serve as a predictor of individual BMI performance and assist in the improvement of general BMI performance.

CONCLUSION

We have developed an ECoG-based real-time BMI system and the first prototype of a fully implantable wireless system. The ECoG-based real-time BMI system successfully provided voluntary control over the grasping and opening of a robotic hand. A fully implantable wireless system is indispensable for the clinical application of invasive BMI to reduce the risk of infection. The noninvasive evaluation of an individual BMI performance using an MEG might be useful for determining the surgical indication of invasive BMI treatment.

Figure 8. Neural decoding using magnetoencephalography. A: a typical averaged waveform of a movement-related cortical field. B: The relationship between the neural decoding accuracies and the peak amplitudes of the first component after the movement onset of the movement-related cortical field.

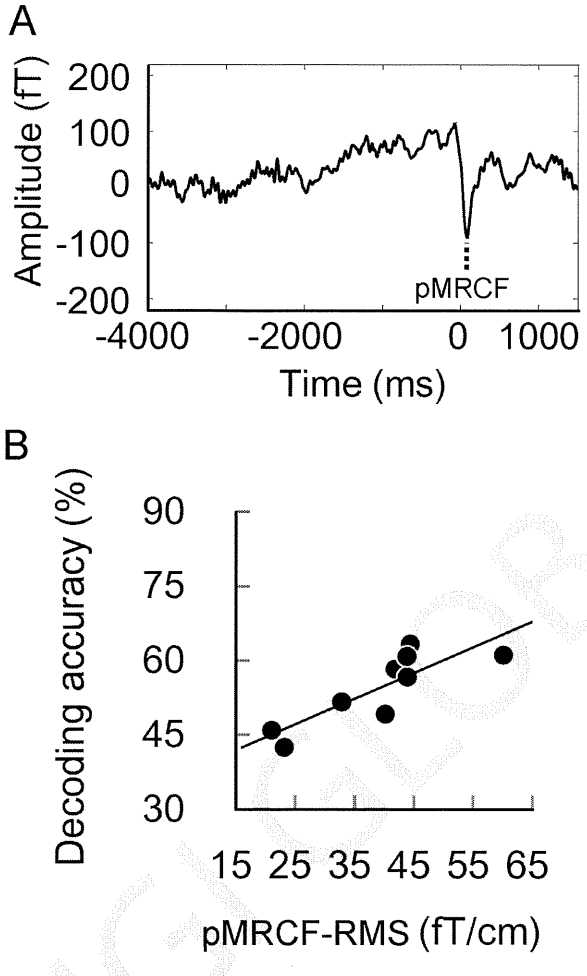

ACKNOWLEDGMENT

This work was supported by the Strategic Research Program for Brain Sciences of MEXT. We would like to acknowledge Atsushi Iwata (A-R-Tec Corp.), Shinichi Morikawa, Yoshihiro Watanabe (Unique Medical), Naohiro Hayaishi (Keisuugiken Corp.), Shinichi Yoshimura, Shuhei Kosaka (Aska Electric Co. Ltd.), and Hirofumi Itoh (Junkosha Inc.) for prototype manufacturing of our implantable system, and we would also like to thank the VLSI Design and Education Center (VDEC) and the University of Tokyo for their help with the chip fabrication program.

REFERENCES

Chao, Z. C., Nagasaka, Y., & Fujii, N. (2010). Long-term asynchronous decoding of arm motion using electrocorticographic signals in monkeys. *Front Neuroengineering*, *3*, 3.

Hirata, M., Matsushita, K., Suzuki, T., Yoshida, T., Sato, F., & Morris, S. (2011). A fully-implantable wireless system for human brain-machine interfaces using brain surface electrodes: W-HERBS. *IEICE Transactions in Communications. E (Norwalk, Conn.)*, *94-B*, 2448–2453.

Hirata, M., Yoshimine, T., Saitoh, Y., Yanagisawa, T., Goto, T., Watanabe, Y., et al. (2010). *US patent Patent No. US7,860,577.*

Kamitani, Y., & Tong, F. (2005). Decoding the visual and subjective contents of the human brain. *Nature Reviews. Neuroscience*, *8*(5), 679–685. doi:10.1038/nn1444

Rathelot, J. A., & Strick, P. L. (2009). Subdivisions of primary motor cortex based on cortico-motoneuronal cells. *Proceedings of the National Academy of Sciences of the United States of America*, *106*(3), 918–923. doi:10.1073/pnas.0808362106

Sugata, H., Goto, T., Hirata, M., Yanagisawa, T., Shayne, M., & Matsushita, K. (2012). Movement-related neuromagnetic fields and performances of single trial classifications. *Neuroreport*, *23*(1), 16–20. doi:10.1097/WNR.0b013e32834d935a

Wolpaw, J. R., Birbaumer, N., McFarland, D. J., Pfurtscheller, G., & Vaughan, T. M. (2002). Brain-computer interfaces for communication and control. *Clinical Neurophysiology*, *113*(6), 767–791. doi:10.1016/S1388-2457(02)00057-3

Yanagisawa, T., Hirata, M., Saitoh, Y., Goto, T., Kishima, H., & Fukuma, R. (2011). Real-time control of a prosthetic hand using human electrocorticography signals. *Journal of Neurosurgery, 114*(6), 1715–1722. doi:10.3171/2011.1.JNS101421

Yanagisawa, T., Hirata, M., Saitoh, Y., Kato, A., Shibuya, D., & Kamitani, Y. (2009). Neural decoding using gyral and intrasulcal electrocorticograms. *NeuroImage, 45*(4), 1099–1106. doi:10.1016/j.neuroimage.2008.12.069

Yanagisawa, T., Hirata, M., Saitoh, Y., Kishima, H., Matsushita, K., Goto, T., et al. (in press). Electrocorticographic control of a prosthetic arm in paralyzed patients. *Annals of Neurology, 71*(3).

Yokoi, H., Kita, K., & Nakamura, T. (2009). Mutually adaptable EMG devices for prosthetic hand. *The International Journal of Factory Automation, Robotics and Soft Computing*, 74-83.

Yoshida, T., Masui, Y., Eki, R., & Iwata, A., M., Y., & Uematsu, K. (2010). A neural recording amplifier with low-frequency noise suppression. *IEICE Transactions in Electrons. E (Norwalk, Conn.), 93-C*, 849–854.

Yoshida, T., Sueishi, K., Iwata, A., Matsushita, K., Hirata, M., & Suzuki, T. (2011). A high-linearity low-noise amplifier with variable bandwidth for neural recording systems. *Japanese Journal of Applied Physics, 50*(4). doi:10.1143/JJAP.50.04DE07

ADDITIONAL READING

Birbaumer, N., & Cohen, L. G. (2007). Brain-computer interfaces: Communication and restoration of movement in paralysis. *The Journal of Physiology, 579*(Pt 3), 621–636. doi:10.1113/jphysiol.2006.125633

Birbaumer, N., Weber, C., Neuper, C., Buch, E., Haapen, K., & Cohen, L. (2006). Physiological regulation of thinking: brain-computer interface (BCI) research. *Progress in Brain Research, 159*, 369–391. doi:10.1016/S0079-6123(06)59024-7

Brunner, P., Bianchi, L., Guger, C., Cincotti, F., & Schalk, G. (2011). Current trends in hardware and software for brain-computer interfaces (BCIs). *Journal of Neural Engineering, 8*(2), 025001. doi:10.1088/1741-2560/8/2/025001

Brunner, P., Ritaccio, A. L., Emrich, J. F., Bischof, H., & Schalk, G. (2011). Rapid communication with a "P300" matrix speller using electrocorticographic signals (ECoG). *Frontiers in Neuroscience, 5*, 5. doi:10.3389/fnins.2011.00005

Buch, E., Weber, C., Cohen, L. G., Braun, C., Dimyan, M. A., & Ard, T. (2008). Think to move: A neuromagnetic brain-computer interface (BCI) system for chronic stroke. *Stroke, 39*(3), 910–917. doi:10.1161/STROKEAHA.107.505313

Felton, E. A., Wilson, J. A., Williams, J. C., & Garell, P. C. (2007). Electrocorticographically controlled brain-computer interfaces using motor and sensory imagery in patients with temporary subdural electrode implants. Report of four cases. *Journal of Neurosurgery, 106*(3), 495–500. doi:10.3171/jns.2007.106.3.495

Guenther, F. H., Brumberg, J. S., Wright, E. J., Nieto-Castanon, A., Tourville, J. A., & Panko, M. (2009). A wireless brain-machine interface for real-time speech synthesis. *PLoS ONE, 4*(12), e8218. doi:10.1371/journal.pone.0008218

Hashimoto, Y., Ushiba, J., Kimura, A., Liu, M., & Tomita, Y. (2010). Change in brain activity through virtual reality-based brain-machine communication in a chronic tetraplegic subject with muscular dystrophy. *BMC Neuroscience, 11*, 117. doi:10.1186/1471-2202-11-117

Hochberg, L. R., Serruya, M. D., Friehs, G. M., Mukand, J. A., Saleh, M., & Caplan, A. H. (2006). Neuronal ensemble control of prosthetic devices by a human with tetraplegia. *Nature*, *442*(7099), 164–171. doi:10.1038/nature04970

Jackson, A., Mavoori, J., & Fetz, E. E. (2006). Long-term motor cortex plasticity induced by an electronic neural implant. *Nature*, *444*(7115), 56–60. doi:10.1038/nature05226

Jarosiewicz, B., Chase, S. M., Fraser, G. W., Velliste, M., Kass, R. E., & Schwartz, A. B. (2008). Functional network reorganization during learning in a brain-computer interface paradigm. *Proceedings of the National Academy of Sciences of the United States of America*, *105*(49), 19486–19491. doi:10.1073/pnas.0808113105

Jochum, T., Denison, T., & Wolf, P. (2009). Integrated circuit amplifiers for multi-electrode intracortical recording. *Journal of Neural Engineering*, *6*(1), 012001. doi:10.1088/1741-2560/6/1/012001

Kellis, S. S., House, P. A., Thomson, K. E., Brown, R., & Greger, B. (2009). Human neocortical electrical activity recorded on nonpenetrating microwire arrays: applicability for neuroprostheses. *Neurosurgical Focus*, *27*(1), E9. doi:10.3171/2009.4.FOCUS0974

Krusienski, D. J., Grosse-Wentrup, M., Galan, F., Coyle, D., Miller, K. J., & Forney, E. (2011). Critical issues in state-of-the-art brain-computer interface signal processing. *Journal of Neural Engineering*, *8*(2), 025002. doi:10.1088/1741-2560/8/2/025002

Kubanek, J., Miller, K. J., Ojemann, J. G., Wolpaw, J. R., & Schalk, G. (2009). Decoding flexion of individual fingers using electrocorticographic signals in humans. *Journal of Neural Engineering*, *6*(6), 66001. doi:10.1088/1741-2560/6/6/066001

Lebedev, M. A., & Nicolelis, M. A. (2006). Brain-machine interfaces: Past, present and future. *Trends in Neurosciences*, *29*(9), 536–546. doi:10.1016/j.tins.2006.07.004

Leuthardt, E. C., Gaona, C., Sharma, M., Szrama, N., Roland, J., & Freudenberg, Z. (2011). Using the electrocorticographic speech network to control a brain-computer interface in humans. *Journal of Neural Engineering*, *8*(3), 036004. doi:10.1088/1741-2560/8/3/036004

McFarland, D. J., Krusienski, D. J., & Wolpaw, J. R. (2006). Brain-computer interface signal processing at the Wadsworth Center: Mu and sensorimotor beta rhythms. *Progress in Brain Research*, *159*, 411–419. doi:10.1016/S0079-6123(06)59026-0

Mellinger, J., Schalk, G., Braun, C., Preissl, H., Rosenstiel, W., & Birbaumer, N. (2007). An MEG-based brain-computer interface (BCI). *NeuroImage*, *36*(3), 581–593. doi:10.1016/j.neuroimage.2007.03.019

Miller, K. J. (2010). Broadband spectral change: evidence for a macroscale correlate of population firing rate? *The Journal of Neuroscience*, *30*(19), 6477–6479. doi:10.1523/JNEUROSCI.6401-09.2010

Miller, K. J., Abel, T. J., Hebb, A. O., & Ojemann, J. G. (2011). Reorganization of large-scale physiology in hand motor cortex following hemispheric stroke. *Neurology*, *76*(10), 927–929. doi:10.1212/WNL.0b013e31820f8583

Miller, K. J., Leuthardt, E. C., Schalk, G., Rao, R. P., Anderson, N. R., & Moran, D. W. (2007). Spectral changes in cortical surface potentials during motor movement. *The Journal of Neuroscience*, *27*(9), 2424–2432. doi:10.1523/JNEUROSCI.3886-06.2007

Miller, K. J., Schalk, G., Fetz, E. E., den Nijs, M., Ojemann, J. G., & Rao, R. P. (2010). Cortical activity during motor execution, motor imagery, and imagery-based online feedback. *Proceedings of the National Academy of Sciences of the United States of America*, *107*(9), 4430–4435. doi:10.1073/pnas.0913697107

Miller, K. J., Zanos, S., Fetz, E. E., den Nijs, M., & Ojemann, J. G. (2009). Decoupling the cortical power spectrum reveals real-time representation of individual finger movements in humans. *The Journal of Neuroscience*, *29*(10), 3132–3137. doi:10.1523/JNEUROSCI.5506-08.2009

Miyawaki, Y., Uchida, H., Yamashita, O., Sato, M. A., Morito, Y., & Tanabe, H. C. (2008). Visual image reconstruction from human brain activity using a combination of multiscale local image decoders. *Neuron*, *60*(5), 915–929. doi:10.1016/j.neuron.2008.11.004

Murguialday, A. R., Hill, J., Bensch, M., Martens, S., Halder, S., & Nijboer, F. (2011). Transition from the locked in to the completely locked-in state: a physiological analysis. *Clinical Neurophysiology*, *122*(5), 925–933. doi:10.1016/j.clinph.2010.08.019

Musallam, S., Bak, M. J., Troyk, P. R., & Andersen, R. A. (2007). A floating metal microelectrode array for chronic implantation. *Journal of Neuroscience Methods*, *160*(1), 122–127. doi:10.1016/j.jneumeth.2006.09.005

Pei, X., Leuthardt, E. C., Gaona, C. M., Brunner, P., Wolpaw, J. R., & Schalk, G. (2011). Spatiotemporal dynamics of electrocorticographic high gamma activity during overt and covert word repetition. *NeuroImage*, *54*(4), 2960–2972. doi:10.1016/j.neuroimage.2010.10.029

Pistohl, T., Ball, T., Schulze-Bonhage, A., Aertsen, A., & Mehring, C. (2008). Prediction of arm movement trajectories from ECoG-recordings in humans. *Journal of Neuroscience Methods*, *167*(1), 105–114. doi:10.1016/j.jneumeth.2007.10.001

Rickert, J., Oliveira, S. C., Vaadia, E., Aertsen, A., Rotter, S., & Mehring, C. (2005). Encoding of movement direction in different frequency ranges of motor cortical local field potentials. *The Journal of Neuroscience*, *25*(39), 8815–8824. doi:10.1523/JNEUROSCI.0816-05.2005

Sato, M. A., Yoshioka, T., Kajihara, S., Toyama, K., Goda, N., & Doya, K. (2004). Hierarchical Bayesian estimation for MEG inverse problem. *NeuroImage*, *23*(3), 806–826. doi:10.1016/j.neuroimage.2004.06.037

Schalk, G. (2010). Can electrocorticography (ECoG) support robust and powerful brain-computer interfaces? *Frontiers in Neuroengineering*, *3*, 9.

Schalk, G., Kubanek, J., Miller, K. J., Anderson, N. R., Leuthardt, E. C., & Ojemann, J. G. (2007). Decoding two-dimensional movement trajectories using electrocorticographic signals in humans. *Journal of Neural Engineering*, *4*(3), 264–275. doi:10.1088/1741-2560/4/3/012

Schalk, G., Miller, K. J., Anderson, N. R., Wilson, J. A., Smyth, M. D., & Ojemann, J. G. (2008). Two-dimensional movement control using electrocorticographic signals in humans. *Journal of Neural Engineering*, *5*(1), 75–84. doi:10.1088/1741-2560/5/1/008

Schwartz, A. B. (2004). Cortical neural prosthetics. *Annual Review of Neuroscience*, *27*, 487–507. doi:10.1146/annurev.neuro.27.070203.144233

Schwartz, A. B., Cui, X. T., Weber, D. J., & Moran, D. W. (2006). Brain-controlled interfaces: Movement restoration with neural prosthetics. *Neuron*, *52*(1), 205–220. doi:10.1016/j.neuron.2006.09.019

Schwartz, A. B., Moran, D. W., & Reina, G. A. (2004). Differential representation of perception and action in the frontal cortex. *Science*, *303*(5656), 380–383. doi:10.1126/science.1087788

Shenoy, P., Miller, K. J., Ojemann, J. G., & Rao, R. P. (2008). Generalized features for electrocorticographic BCIs. *IEEE Transactions on Bio-Medical Engineering*, *55*(1), 273–280. doi:10.1109/TBME.2007.903528

Toda, A., Imamizu, H., Kawato, M., & Sato, M. A. (2011). Reconstruction of two-dimensional movement trajectories from selected magneto-encephalography cortical currents by combined sparse Bayesian methods. *NeuroImage*, *54*(2), 892–905. doi:10.1016/j.neuroimage.2010.09.057

Ushiba, J. (2010). Brain-machine interface--Current status and future prospects. *Brain Nerve*, *62*(2), 101–111.

Vansteensel, M. J., Hermes, D., Aarnoutse, E. J., Bleichner, M. G., Schalk, G., & van Rijen, P. C. (2010). Brain-computer interfacing based on cognitive control. *Annals of Neurology*, *67*(6), 809–816.

Velliste, M., Perel, S., Spalding, M. C., Whitford, A. S., & Schwartz, A. B. (2008). Cortical control of a prosthetic arm for self-feeding. *Nature*, *453*(7198), 1098–1101. doi:10.1038/nature06996

Waldert, S., Pistohl, T., Braun, C., Ball, T., Aertsen, A., & Mehring, C. (2009). A review on directional information in neural signals for brain-machine interfaces. *The Journal of Physiology*, *103*(3-5), 244–254.

Waldert, S., Preissl, H., Demandt, E., Braun, C., Birbaumer, N., & Aertsen, A. (2008). Hand movement direction decoded from MEG and EEG. *The Journal of Neuroscience*, *28*(4), 1000–1008. doi:10.1523/JNEUROSCI.5171-07.2008

Whittingstall, K., & Logothetis, N. K. (2009). Frequency-band coupling in surface EEG reflects spiking activity in monkey visual cortex. *Neuron*, *64*(2), 281–289. doi:10.1016/j.neuron.2009.08.016

Wolpaw, J. R. (2007). Brain-computer interfaces as new brain output pathways. *The Journal of Physiology*, *579*(Pt 3), 613–619. doi:10.1113/jphysiol.2006.125948

Wolpaw, J. R., & McFarland, D. J. (2004). Control of a two-dimensional movement signal by a noninvasive brain-computer interface in humans. *Proceedings of the National Academy of Sciences of the United States of America*, *101*(51), 17849–17854. doi:10.1073/pnas.0403504101

Wu, M., Wisneski, K., Schalk, G., Sharma, M., Roland, J., & Breshears, J. (2010). Electrocorticographic frequency alteration mapping for extraoperative localization of speech cortex. *Neurosurgery*, *66*(2), E407–E409. doi:10.1227/01.NEU.0000345352.13696.6F

Yamashita, O., Sato, M. A., Yoshioka, T., Tong, F., & Kamitani, Y. (2008). Sparse estimation automatically selects voxels relevant for the decoding of fMRI activity patterns. *NeuroImage*, *42*(4), 1414–1429. doi:10.1016/j.neuroimage.2008.05.050

KEY TERMS AND DEFINITIONS

Brain Surface Electrodes: Electrodes that are directly placed on the brain surface.

Brain-Machine Interface: A man-machine interface, which enables us to control machines and to communicate with others without the use of input devices, but through the direct use of brain signals alone.

Implantable Device: A medical device implanted within the body.

Motor Restoration: Recovery of neural motor function.

Neural Decoding: Decoding neural signals.

Prosthetic Arm: An artificial robotic arm that substitutes for a missing arm.

Real Time: To respond on the order of milliseconds and at times, microseconds.

INVITED PAPER

Clinical application of neuromagnetic recordings: from functional imaging to neural decoding

Masayuki HIRATA[†], *Nonmembers and* **Toshiki YOSHIMINE**[††], *Nonmembers*

SUMMARY Magnetoencephalography (MEG) measures very weak neuromagnetic signals using SQUID sensors. Standard MEG analyses include averaged waveforms, isofield maps and equivalent current dipoles. Beamforming MEG analyses provide us with frequency-dependent spatiotemporal information about the cerebral oscillatory changes related to not only somatosensory processing but also language processing. Language dominance is able to be evaluated using laterality of power attenuation in the low γ band in the frontal area. Neuromagnetic signals of the unilateral upper movements are able to be decoded using a support vector machine.

key words: *Magnetoencephalography, oscillation, neuroimaging, beamformer, neural decoding*

1. Introduction

Intensity of neuromagnetic signals ranges from 10^{-14} tesla (T) to 10^{-12} T, which is approximately billionth part of earth's magnetism and millionth part of that of magnetic noises in cities. Magnetoencephalography (MEG) measures such very weak neuromagnetic signals directly related to intracellular electrical currents caused by neuronal activities, so that MEG enables us to detect neural activities with temporal resolution as high as millisecond order [1]. SQUID sensors are used as neuromagnetic sensors, which have sufficient sensitivity as high as approximately 10 fT / √Hz (white noise). MEG estimates neural current generators more precisely than electroencephalography (EEG). Because magnetic reluctance of the body tissues is uniform, neuromagnetic signals fit better with simple conductance models of the skull for analyses, whereas electric conductance of the body tissues is not uniform. Utilizing the precision, MEG is used for neuroscientific researches and neurological evaluations such as functional neuroimaging and evaluation of epileptic foci [2]. Most recently, neural decoding techniques have been introduced in the field of MEG to facilitate the effectiveness of neurorehabilitation [3].

In this paper, we describe the recent progress in our MEG research on clinical application regarding functional neuroimaging and neural decoding based on neuromagnetic recordings.

Manuscript received July xx, 2012.
Manuscript revised March xx, 2012.

†The authors are with Department of Neurosurgery, Osaka University Medical School, Suita-shi, Osaka, 565-0871 Japan.

2. Backgrounds

2.1 Cerebral oscillatory changes

Synchronous oscillations in specific frequency bands such as alpha waves are well known as basic brain rhythms. These basic rhythms change signal power due to brain activation. Event-related desynchronization (ERD) is an attenuation of the oscillation amplitude of a specific frequency band that occurs in relation to specific neural activities [4]. The opposite phenomenon, event-related synchronization (ERS), is an increase in that amplitude [5].

Synchronous oscillations can be measured using EEG, MEG and electrocorticography (ECoG) which is neural activities recorded from electrodes directly placed on the brain surface. Fig. 1 shows the time-frequency spectrograms of ECoGs during right hand grasping. The ECoGs are recorded from grid electrodes placed over the left sensorimotor areas of the human brain. ERDs are observed in the 8 – 25Hz (α and β bands) over the sensorimotor areas broadly, whereas ERSs are observed in the 50 – 200Hz (high γ band) in the sensorimotor areas more focally. Regarding time domain also, ERDs occur 500 – 1000 ms prior to muscle contraction and sustained even after the end of muscle contraction, whereas ERSs occurs more strictly during muscle contraction. ERS in the high γ band is known to reflect functional localization of the brain better than ERD in the α and β bands. These oscillatory changes during movements are called as movement-related cerebral oscillatory changes. Cerebral oscillatory changes are observed not only during movements, but also during language activities, sensory processing and mental concentration. ECoG provides us with precise neural activities directly from brain surface electrodes, but needs brain surgery. MEG is noninvasive as well as precise in functional localization.